

Characterization of an Ar/N₂ reactive amplified magnetron discharges by Atomic Absorption Spectroscopy and Glow Discharge Mass Spectrometry

S. Konstantinidis^{a,*}, A. Ricard^b, R. Snyders^a, H. Vandeparre^a, J.P. Dauchot^a, M. Hecq^a

^aLab. of Inorganic and Analytical Chemistry, University of Mons-Hainaut, Materia Nova, Av. Copernic, Parc Initialis, 7000 Mons, Belgium

^bCPAT, Univ. Paul Sabatier, 118 route de Narbonne, 31062 Toulouse, France

Available online 26 April 2005

Abstract

The aim of this paper is the characterization of an inductively amplified magnetron discharge running in reactive mode (Ar/N₂ gas mixture with titanium target) using Atomic Absorption Spectroscopy and Glow Discharge Mass Spectrometry. The first technique gives access to absolute densities of sputtered metal, usually neutrals. In this paper, ionic titanium densities are also estimated thanks to a pulsed hollow cathode lamp used as optical source for absorption measurements. The second technique deals with the relative behaviour of ions extracted from the plasma.

At a given pressure, both diagnostic methods are correlated in describing the evolution of the metallic species as the target surface evolves, with the nitrogen content, from the metallic to the poisoned state. The transition is marked by the decrease of titanium neutral (measured by absorption spectroscopy) and relative ionic densities (by mass spectrometry). At 0.7 Pa, the transition happens for a gas mixture containing 6% of nitrogen. It happens for 4% of nitrogen at higher pressure (3.9 Pa). It confirms the validity of mass spectrometry to qualitatively follow titanium neutral density in reactive mode. Nevertheless, both techniques are not correlated in describing the evolution of Ti⁺ and Ti as the total pressure increases from 0.7 to 9.1 Pa.

© 2005 Elsevier B.V. All rights reserved.

Keywords: Mass spectrometry; Absorption spectroscopy; Amplified magnetron

1. Introduction

Glow Discharge Mass Spectrometry (GDMS) is often used as a magnetron discharges diagnostic tool [1]. This technique is especially relevant in the case of reactive magnetron discharges, when a reactive gas, such as nitrogen or oxygen, is mixed to the sputtering gas. The plasma composition can be analysed and correlated to the deposited thin film properties. But only ions produced in the plasma are detected and the signal is relative to mass spectrometer parameters (i.e. ion detector high voltage supply).

On the other hand, Atomic Absorption Spectroscopy (AAS) gives access to absolute densities of neutral species [2]. The field of this technique has been enlarged to the detection of metallic ions produced in an RF amplified

magnetron system by pulsing the hollow cathode lamp power supply used as optical source [3,4].

In this study, we propose to compare densities (ions and neutrals), as obtained by AAS and GDMS, in the case of an amplified magnetron discharge in pure argon and in the Ti–Ar/N₂ system, for titanium nitride deposition. The ionization fraction of the metallic species is varied in this experiment by the power transmitted to the plasma electrons by means of a radiofrequency (RF) power supplied copper coil.

2. Experimental setup

The experimental setup used for pulsed absorption spectroscopy is presented in Refs. [3,4]. The mass spectrometer equipped with energy resolved capability is described in Ref. [5]. Fig. 1 presents a top view of the 35 cm high stainless steel deposition chamber and the spatial layout of both diagnostic tools.

* Corresponding author. Tel.: +32 65 37 38 45; fax: +32 65 37 38 41.

E-mail address: stephanos.konstantinidis@umh.ac.be
(S. Konstantinidis).

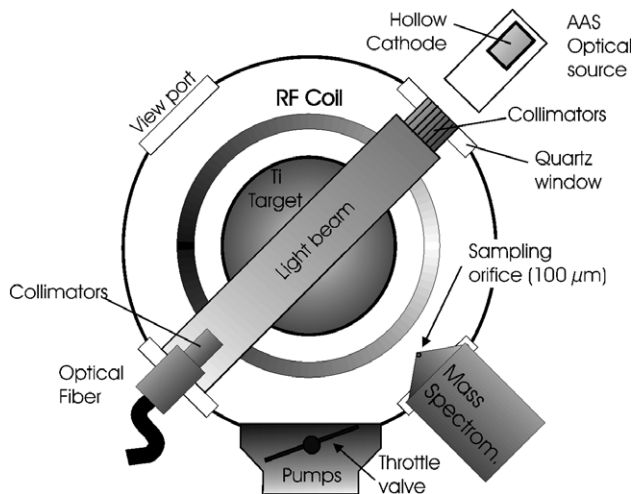


Fig. 1. Vacuum chamber (top view) and schematic representation of the light beam crossing the vacuum chamber and the GDM Spectrometer sampling orifice.

The extraction orifice used for the mass spectrometry diagnostic is positioned about 20 cm away from the target surface. The light beam emitted by the optical source crosses the reactor along its diameter which is 25 cm wide.

The GDMS and the AAS measurements are simultaneously realized. Absorption coefficients, mass and energy spectra are recorded for different compositions and pressures (0.7 to 9.1 Pa) of the discharge gas. The nitrogen fraction in the plasma is varied from 0 up to 10%, in a way to cross the metal-poisoned regime boundary. The total gas flow is kept at a constant value of 40 sccm. Ion signal deduced from GDMS experiments is calculated via the Ion Energy Distribution Function (IEDF) integration.

The magnetron cathode is a titanium disk (10 cm diam.). The power supplied to the magnetron cathode (P_{dc} —Direct Current) is 500 W. The copper coil, for metallic vapour

ionization, is located 4 cm above the sputtering target. The plane, where both diagnostics are done, is located approximately 1 cm above the coil plane, between the coil and the substrate holder. The power applied to the RF coil (P_{rf}) can be increased up to 500 W.

3. Densities of Ti and Ti^+ in Ar by AAS and GDMS

As a first step, the densities of Ti and Ti^+ have been determined by resonant AAS for a constant DC power of 500 W, following the Ar gas pressure. The diagnostic method is described in Refs. [2,3] where results on Ti and Ti^+ in ground and metastable states are reported at a constant gas pressure of 3.9 Pa, for the DC and RF powers of 500 W. In the present paper, the Ti and Ti^+ density measurements have been extended to the 0.7–9.1 Pa pressure range, in pure magnetron discharge.

As mentioned in Ref. [3], it is necessary to know the Doppler profile of plasma lines to perform AAS. The Doppler line broadenings have been determined, at a pressure higher than 3.9 Pa, from the rotational temperatures of N_2 in Ar. As indicated in Refs. [6,7], the thermalization of Ar and Ti species is achieved 5 cm above the cathode for such high pressures. At a lower gas pressure, the sputtered Ti atoms should be no longer thermalized with the argon atoms. For example, from Ref. [6], a thermalization distance of 5 cm is calculated at 0.7 Pa. But from Ref. [7], the Ti atom energy at 0.7 Pa is calculated to be ~ 1.5 eV at 5 cm.

The variation of the Ti ground state (a^3F_2) atom density versus the Ar gas pressure is reproduced in Fig. 2 for $P_{dc}=500$ W and $P_{rf}=0$ W. At pressure higher than 3.9 Pa, the Ti temperature is taken equal to the room gas temperature $T=300$ K, as determined in Ref. [2].

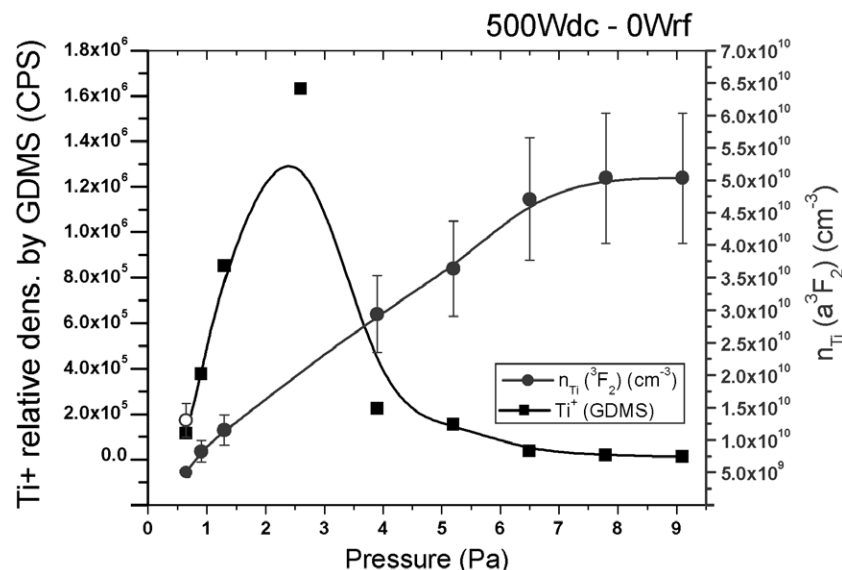


Fig. 2. GDMS and AAS signals versus working pressure (pure Ar atmosphere, 500 Wdc). Error is estimated to be 20%.

At 0.7 Pa, the Ti atoms are considered as being not thermalized in the direction perpendicular to the cathode, thus perpendicular to the optical observation. In consequence, the Doppler effect can be considered as nearly absent (only a Doppler shift should be observed in the Ti beam direction). A density value of $0.5 \times 10^{10} \text{ cm}^{-3}$ is calculated by taking $T=300 \text{ K}$ for the Ti atoms at 0.7 Pa. It can be indicated that with an unrealistic Doppler temperature of 1.5 eV, the density of Ti atoms should be $1.3 \times 10^{10} \text{ cm}^{-3}$ (open disk in Fig. 2).

The variation of the Ti^+ signal as obtained by GDMS versus the gas pressure is also reproduced in Fig. 2. The settings used for the mass spectrometer ion counting are left unchanged for all the measurements. It is clear that the Ti^+ relative density obtained by GDMS is not related to the Ti atom density obtained by AAS. Between 3.9 and 9.1 Pa, the Ti^+ (GDMS) and the Ti (AAS) vary in opposite way.

The Ti^+ ion density measured by AAS, using the transition at 338.4 nm, is reported in Fig. 3 with $P_{\text{rf}}=0 \text{ W}$ and $P_{\text{rf}}=500 \text{ W}$. This transition occurs between the following energy levels $^4\text{F}_{3/2} \rightarrow ^4\text{G}_{5/2}$ and is characterized by an oscillator strength $f=0.19$. The Ti^+ (AAS) density also increases with pressure, as for the Ti.

The ions are believed to behave as neutrals, in an electric field free region. The Doppler profile chosen for Ti ions corresponds to a temperature of 300 K at 1.3 Pa, whatever the plasma is amplified or not. At medium pressure (3.9 Pa), the temperature is 300 K ($P_{\text{rf}}=0 \text{ W}$) and 500 K ($P_{\text{rf}}=500 \text{ W}$). For higher pressure (9.1 Pa), the same temperatures are chosen.

Mao et al. [8] present an increase in gas temperature from 600 K to 1000 K as pressure evolves from 2 to 3.3 Pa, at constant RF power (1 kWrf). So, density estimation

presented in Fig. 3 is also presented using 750 K at 9.1 Pa, 500 Wrf (black square).

It can be concluded by comparing Figs. 2 and 3 that the measurements by AAS, being located near the substrate at 5 cm of the magnetron cathode, do not agree with the GDMS in following the variations of Ti and Ti^+ densities in the specified pressure range. The main reason is that, in ASS, the density is measured on a volume corresponding to the path of the light beam through the plasma while, for GDMS, the detection is made via the sampling orifice which is located far from the cathode (20 cm) as presented in Fig. 1. Then, as the pressure increases, the sputtered titanium species form a cloud above the target surface and we observe a monotonic increase of Ti and Ti^+ densities with AAS. In the case of GDMS, the signal passes through a maximum value. Firstly, the Ti^+ signal increases with pressure because of the increased ionization probability of titanium atoms which are slowed down due to the augmented number of collisions. But this effect is compensated by the reduction of the collection of ions because of the small mean free path at higher pressures.

4. Densities of Ti and Ti^+ in Ar– N_2 discharges by AAS and GDMS

Titanium neutral and ionic signals, respectively obtained by AAS and GDMS, are represented as a function of nitrogen percentage in the gas mixture in Fig. 4a and b at two fixed total pressures. A drop of densities is observed for 6% N_2 at 0.7 Pa and 4% N_2 at 3.9 Pa. Such N_2 percentages correspond to the transition between the metal and poisoned (nitrided) modes of the cathode [1,9]. It is noted that such

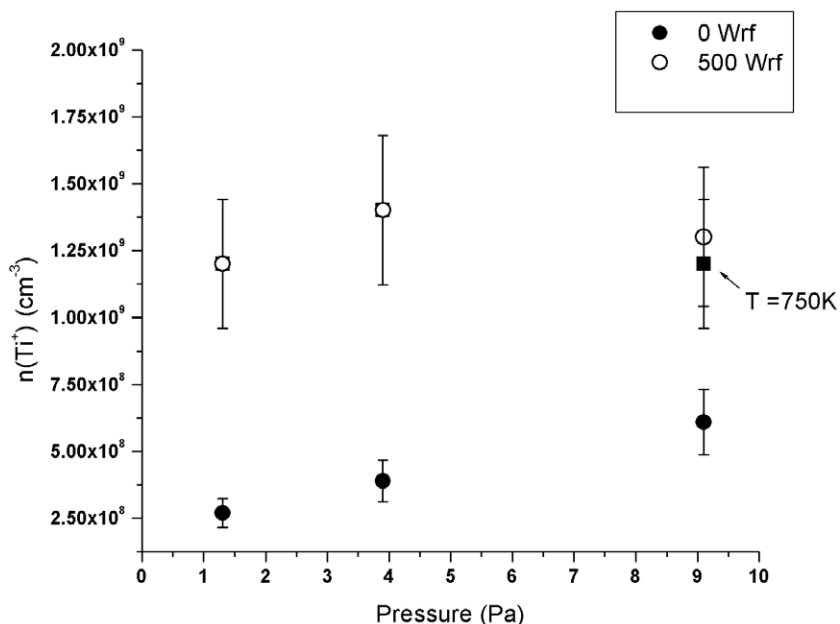


Fig. 3. Ti ions density versus working pressure, with (500 Wrf—white symbols) and without (0 Wrf—black symbols) RF amplification. See text for explanation relative to the square point. Error is estimated to be 20%.

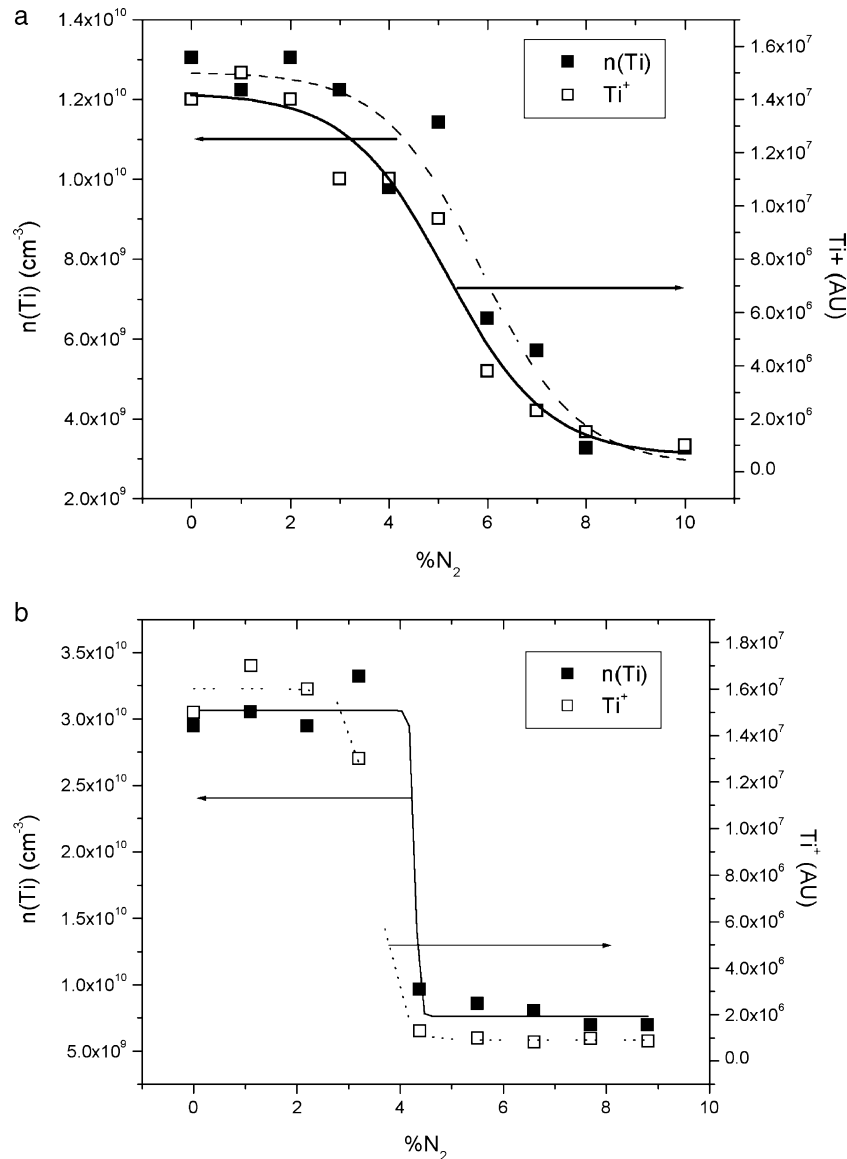


Fig. 4. Evolution of Ti densities determined by AAS (black squares) and Ti^+ relative densities determined by GDMS (white squares) with nitrogen flow at (a) 0.7 Pa, 0 Wrf and (b) 3.9 Pa, 0 Wrf.

transitions are, for a given pressure, observed both with GDMS and AAS for the same nitrogen contents.

Different causes can explain the origin of this density reduction. Firstly, once the target is nitrated, the secondary electron emission coefficient decreases and consequently, both the discharge current and voltage are modified [5]. The discharge current diminishes and the voltage, to keep the target power constant (500 W), increases. For example, with 500 Wdc, 0 Wrf, 3.9 Pa, the discharge voltage goes from 265 V (0% N₂) to 330 V (5% N₂). But the sputtering yield increases sub-linearly with the energy of the ions. Secondly, the nitrogen atomic and molecular ions, because they are no more pumped down by the getter effect, become more involved in the physical sputtering phenomenon; but they are less efficient than argon ions for sputtering due to their smaller mass. Furthermore, the sputtering yield decreases

also because of the chemical nature of the target top layer. The sputtering yield of titanium nitride is lower than titanium. The probability to sputter titanium is also reduced because, at the extreme surface, the titanium atoms are replaced by nitrogen atoms and because the probability to sputter titanium nitride clusters instead of titanium atoms increases [5]. Therefore, as a global consequence, the amount of titanium in the plasma declines.

By comparing Fig. 4a and b, one can see that the transition appears at a lower reactive gas partial flow at 3.9 Pa because the nitrogen partial pressure, which is the effective parameter to take into account for target poisoning [1], is higher than at 0.7 Pa.

When the magnetron discharge is amplified with 500 Wrf on the coil (Fig. 5), the transition is also observed simultaneously with AAS and GDMS. The titanium neutral

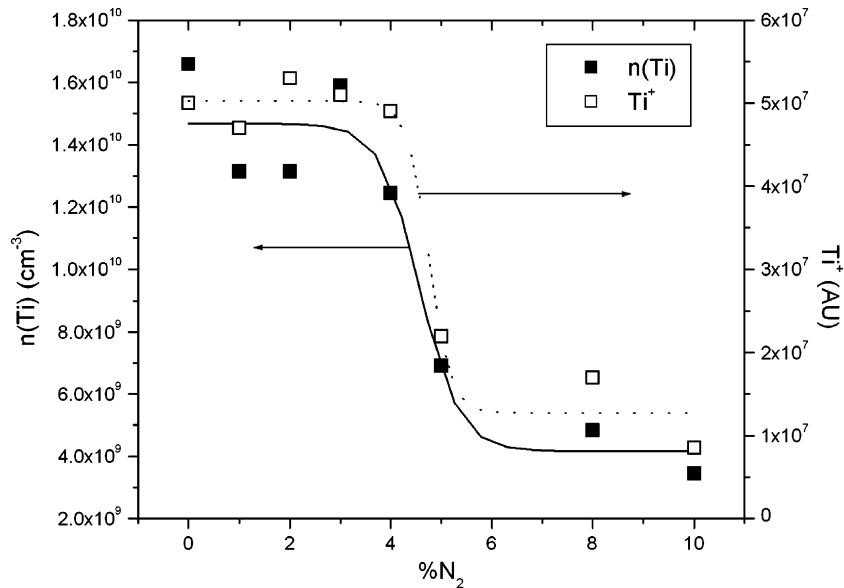


Fig. 5. Evolution of Ti densities estimated by AAS (black squares) and Ti^+ relative densities obtained by GDMS (white squares) with nitrogen flow (3.9 Pa, 500 Wrf).

densities are lower than those presented in Fig. 4b, as a result of the metallic vapour ionization by the dense secondary plasma produced by the RF coil.

In conclusion, those measures confirms the validity of GDMS to qualitatively follow the evolution of titanium neutrals species, when a magnetron, amplified or not, runs in reactive mode.

5. Conclusions

In this paper, we have compared the signals derived from two different diagnostic techniques: Absorption Spectroscopy deals with absolute metal densities and Mass Spectrometry is employed to detect ions extracted from the plasma.

The evolution of both signals does not correspond as the working pressure evolves from 0.7 to 9.1 Pa. Ion sampling by the mass spectrometer is diffusion limited at high pressures. The mass spectrometer signal is declining while the titanium neutrals and ionic densities, determined by AAS, are increasing.

At a given pressure (0.7 and 3.9 Pa), both diagnostics are correlated. They follow the density reduction caused by the so-called target poisoning as the nitrogen mass flow increases. The same results are obtained when the RF antenna amplifies the plasma. Those measures confirm the

validity of GDMS to qualitatively follow the evolution of titanium neutrals species, when a magnetron, amplified or not, runs in reactive mode.

Acknowledgement

The author would like to thank the “Fonds pour la formation à la Recherche dans l’Industrie et dans l’Agriculture (FRRIA)” for financial support.

References

- [1] R. Snyders, R. Gouttebaron, J.P. Dauchot, M. Hecq, *J. Anal. At. Spectrom.* 18 (2003) 618.
- [2] A. Ricard, C. Nouvellon, S. Konstantinidis, J.P. Dauchot, M. Wautelet, M. Hecq, *J. Vac. Sci. Technol., A* 20 (4) (2002) 1488.
- [3] S. Konstantinidis, A. Ricard, M. Ganciu, J.P. Dauchot, C. Ranea, M. Hecq, *J. Appl. Phys.* 95 (6) (2004) 2900.
- [4] S. Konstantinidis, A. Ricard, M. Ganciu, J.P. Dauchot, M. Wautelet, M. Hecq, *Proceedings of the 46th Society of Vacuum Coaters Technical Conference* (San Francisco, USA, May 2003), 2003, p. 475.
- [5] S. Konstantinidis, C. Nouvellon, J.P. Dauchot, M. Wautelet, M. Hecq, *Surf. Coat. Technol.* 174–175 (2003) 100.
- [6] W.D. Westwood, *J. Vac. Sci. Technol., A* (15) (1978) 1.
- [7] F. Clenet, P.H. Briaud, G. Lemprière, G. Turban, *Thin Solid Films* 346 (1999) 290.
- [8] D. Mao, K. Tao, J. Hopwood, *J. Vac. Sci. Technol., A* (20) (2002) 379.
- [9] D. Depla, R. De Gryse, *Vacuum* 69 (2003) 529.